IEEE Access
Multidisciplinary | Rapid Review | Open Access Journal

Received April 24, 2020, accepted May 10, 2020, date of publication May 25, 2020, date of current version June 16, 2020.

Digital Object Identifier 10.1109/ACCESS.2020.2996028

Evaluating and Reducing the Influence of Scalp Dehydration in the Monitoring of Intracranial Dehydration Using Electrical Impedance Tomography

HAOTING LI, LU CAO, CANHUA XU, BIN YANG, MENG DAI, XUETAO SHI, XIUZHEN DONG (Member, IEEE), AND FENG FU

School of Biomedical Engineering, Air Force Medical University (Fourth Military Medical University), Xi'an 710032, China

Corresponding authors: Xiuzhen Dong (dongxiuzhen@fmmu.edu.cn) and Feng Fu (fengfu@fmmu.edu.cn)

This work was supported in part by the Project of the National Natural Science Foundation of China under Grant 51837011, in part by the National Natural Science Foundation of China under Grant 31771073, and in part by the National Natural Science Foundation of China under Grant 61771475.

ABSTRACT Dehydration treatment is commonly applied to treat intracranial hypertension. We previously utilized electrical impedance tomography (EIT) for noninvasively monitoring the efficacy of dehydration treatments and found it could provide references for the rational use of dehydrating drugs. In addition to brain tissues, scalp undergoes dehydration and can cause impedance changes, which may hamper the monitoring results of intracranial dehydration through EIT. To address this problem, we first conducted simulation and animal experiments to evaluate the impact of scalp dehydration on the monitoring results of EIT during dehydration treatments. With the priori of the spatial distribution of brain structures and the statistical results of the contribution of scalp dehydration to the intracranial reconstructed values of the EIT images obtained from animal experiments, we then proposed a weighting algorithm to reduce the impact of scalp dehydration. The experimental results showed that scalp impedance changes would to some extent reduce the accuracy of EIT in imaging intracranial resistive perturbation and account for 16.7% in overall changes of EIT signal. With the modified algorithm, 69.6% of reconstructed values of scalp dehydration in EIT images were eliminated. And the image contrast (IC) of reconstructed EIT images was improved by 21.0%. Therefore, we conclude that scalp dehydration influences the accuracy of EIT in reflecting intracranial dehydration and our proposed method can reduce the impacts of scalp dehydration.

INDEX TERMS Intracranial hypertension, electrical impedance tomography, dehydration treatment, modified reconstruction algorithm, rabbit model.

I. INTRODUCTION

Electrical impedance tomography is a non-invasive, low cost and real time imaging method, which has been widely studied in biomedical fields including in the imaging of ventilation, brain function, brain injury, and gastric motility [1]–[4]. Our group had been working on brain EIT and explored many possible clinical applications for it.

Intracranial hypertension is a severe pathology in brain which can cause reduced cerebral blood supply, neurological damage and even death [5]. Dehydration treatment is commonly applied to reduce elevated intracranial pressure (ICP) [6]. However, patients may have different sensitivities to dehydration drugs. The improper use of drugs can not only cause problems in controlling the ICP but also lead to side effects. For example, the repeated use of mannitol with excessive dosage may harm renal function, cause ''rebound'' phenomenon, and aggravate cerebral edema [7]. Hence, a device that can monitor the efficacy of dehydration treatments is required to provide references for personalized medication [8].

In [9], Fu explored the use of dynamic EIT to monitor brain impedance changes of patients with dehydration treatments. The results demonstrated that by classifying the variation

The associate editor coordinating the review of this manuscript and approving it for publication was Sudipta Roy.

trends in the brain EIT signals, we could evaluate the efficacy of dehydration treatments in reducing ICP and estimate the sensitivities of different patients to mannitol [10], [11]. Additionally, the EIT images showed promise in reflecting the dehydration effects in the different areas of the brain.

In other applications of brain EIT, including imaging brain functions or brain injuries, the resistive perturbations due to physiological or pathological changes occur only inside the brain [12], [13]. But in monitoring dehydration treatments, the scalp itself undergoes dehydration and has impedance changes. Moreover, as brain EIT requires placing electrodes on the scalp for measurement [13], [14], the dehydration results of the scalp will be involved in the monitoring results of brain EIT, which might reduce the accuracy of brain EIT in reflecting intracranial dehydration. To accurately evaluate the position and degree of intracranial dehydration by EIT, it is necessary to evaluate the influence of scalp dehydration and propose methods to reduce its impacts in this study.

To investigate the influence of scalp on the imaging results of EIT, a 3D simulation rabbit model with layer structures was built [15], whereby we could analyze the intracranial current density and compare the imaging results of EIT with and without scalp impedance changes. Then, in animal experiments, we inserted an insulating material between the skull and scalp of a rabbit so that the scalp impedance changes during the dehydration could be solely measured, and the ratio of the scalp measurement in the EIT signals was estimated.

To reduce the influence of scalp dehydration, with the priori of the brain structure, we can eliminate the unwanted reconstruction results in the scalp and skull areas of the EIT images [16]. Subsequently, with the imaging results of the dehydrations of the scalp and the entire brain obtained from animal experiments, we can compare the reconstructed intracranial impedance changes in the EIT images in the above two cases. Thus, the contribution of scalp dehydration to the reconstructed values in the intracranial area of the EIT images can be estimated and used as a scale factor to reduce the impact of the scalp dehydration. Based on the above analysis, we proposed a weighting matrix for the EIT algorithm and tested its performance based on simulation experiments.

The experimental results showed that scalp dehydration can lead to changes in the EIT signals and to some extent affect the accuracy of the EIT in imaging intracranial resistive perturbation. After processing with the modified reconstruction algorithm, the impact of scalp dehydration was reduced, and the EIT could reflect the intracranial dehydration with improved accuracy.

II. MONITORING DEHYDRATION TREATMENT WITH BRAIN EIT

In monitoring dehydration treatments for patients with cerebral hypertension, as displayed in Fig. 1(a), a set of EIT electrodes was evenly placed on the scalp of the patients, through which safe currents (1 mA, 50 kHz) were injected into patients and the responding voltage changes

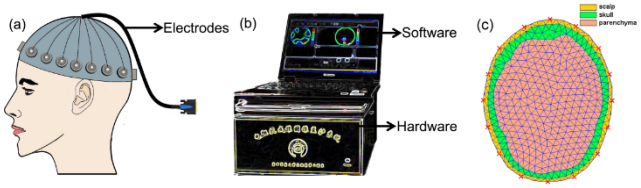

FIGURE 1. Illustration of the brain EIT system for monitoring dehydration treatments: (a) EIT electrodes, (b) Hardware and software (c) Finite element head model for image reconstruction.

were measured based on the instrument FMMU-EIT5 [10], as shown in Fig. 1(b). The measurement accuracy and common mode rejection ratio of this brain EIT system is 0.01% and over 75 dB. For image reconstruction algorithm, we used the optimized NOSER algorithm, which has shown good accuracy for imaging large-area resistive perturbation due to brain dehydration [17]. Fig. 1(c) shows the finite element model (FEM) with brain geometric boundary and three layers for image reconstruction [18]. The imaging speed of EIT in this application was maintained at 1 image per second, and the monitoring last for approximately 3 h. The reference frame was obtained by averaging 200 frames before the infusion of mannitol agent. And regularization parameter was selected using the noise level based method [19].

With the monitoring results of EIT, the total boundary voltage (TBV) and average reconstructed value (ARV) in area Γ were calculated to analyze the efficacy of dehydration treatments.

With the measured boundary voltages, we could calculate the TBV at the time constant t:

$$\mathrm{TBV}(t) = \sum_{i=1}^{n} U_i(t) \tag{1}$$

where $U_i(t)$ is the boundary voltage measured by EIT at the time constant t, and n is the number of elements in $U_i(t)$. In the previous study, we found the classification results of TBV curves of different patients according to their variation trends corresponded to different efficacies of the mannitol in reducing ICP [11].

Then, with the reconstructed EIT images, we define the ARV in area Γ as:

$$\mathrm{ARV}|_\Gamma = (\sum_{i=1}^{m_\Gamma} \delta\rho_i|_\Gamma)/m_\Gamma \tag{2}$$

where m_Γ represents the number of elements in Γ, and $\delta\rho_i|_\Gamma$ is the reconstructed value of the *ith* element in Γ. In mannitol dehydration, $\mathrm{ARV}|_\Gamma$ can be used to analyze the dehydration in Γ.

In dehydration treatments, the reduction of elevated ICP is only related to dehydration of intracranial tissues. However, mannitol would inflow into blood vessels and cause dehydration to all body tissues. The blood vessels of scalp is rich so the scalp will also has dehydration and its impedance changes will be involved into brain EIT images and signals. As dehydration of scalp and intracranial brain tissues occur

simultaneously and their signals can't be discriminated with frequency characters, so the scalp dehydration would disturb EIT in reflecting intracranial dehydration. In the following sections of the study, we will evaluate and reduce the impacts of scalp impedance changes in results of brain EIT in monitoring dehydration treatments.

III. EVALUATION OF THE INFLUENCE OF SCALP DEHYDRATION

In this section, we design simulation and animal experiments to evaluate the impacts of scalp dehydration in monitoring brain dehydration treatments with EIT by answering the two questions:

(1) How do changes in the scalp impedance affect EIT in the imaging of intracranial resistive perturbations?

(2) What is the contribution of impedance changes to the EIT signal in dehydration treatments?

A. THREEE-DIMENSIONAL SIMULATION RABBIT HEAD MODEL

To investigate the influence of scalp dehydration in the imaging results of EIT, we constructed a three-dimensional (3D) FEM rabbit head model, as shown in Fig. 2(a), using COMSOL [15], [18]. It is composed of 20,541 mesh elements and has a three-layer structure, including the scalp, skull, and brain parenchyma. In the 3D rabbit head model, the resistivity values of the scalp, skull, and parenchyma were set to 2.27, 83.3, and 6.71 Ω/m, respectively, by referring to the data provided by Tang [20]. Eight Ag/AgCl electrodes were evenly placed in the form of a ring shape on the scalp. Based on this model, we can increase the impedance of the brain tissues to simulate brain dehydration and generate the simulated EIT data for further analysis. Fig. 2(b) shows the 2D FEM model for image reconstruction. This model has 480 elements, comprising three layers including scalp, skull, and parenchyma.

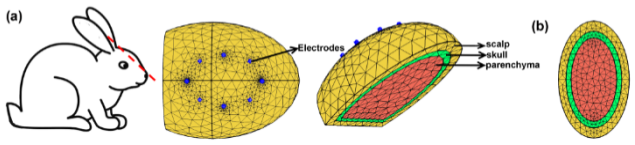

FIGURE 2. Generation of a 3D rabbit head model.

B. SIMULATION EXPERIMENT

Based on the above 3D model, we investigate how scalp impedance changes would influence the imaging results of EIT in monitoring intracranial dehydration treatments.

First, in imaging intracranial dehydration, brain EIT should be sensitive to impedance changes inside the brain. However, the increase of resistivity of scalp due to dehydration may block the flow of the excitation currents into the brain. The detection sensitivity of brain EIT is proportional to current density [21]. So we propose the metric current density (CD) and compare its values with or without increase of impedance changes::

$$CD_i = \frac{\delta V_i}{\rho_i a_i} \tag{3}$$

where CD_i is the current density, δV_i is the drop in voltage, ρ_i is the resistivity, and a_i is the size of the i *th* element.

Second, EIT images are expected to reflect dehydration effects in different areas of the brain. So, we will simulate areas with bad dehydration and compare the imaging results with or without scalp impedance changes. And metrics including image contrast (IC), location error (LE) and Image correlation coefficient (ICC) are introduced to evaluate the quality of reconstructed EIT images [22].

In the reconstructed EIT images, the ARV in the interested area Γ is $\mathrm{ARV}|_\Gamma$ while that of the entire image is $\mathrm{ARV}|_{all}$. Therefore, the IC for Γ can be calculated as:

$$IC_\Gamma = \frac{\mathrm{ARV}|_\Gamma}{\mathrm{ARV}|_{all}} \tag{4}$$

where IC_Γ represents the contrast between the average reconstructed value in Γ and that of the entire area of the image.

The centers of gravity of the Γ in the reference and reconstructed EIT images are denoted by (x^P_{CG}, y^P_{CG}) and (x^T_{CG}, y^T_{CG}), respectively. Accordingly, the LE can be calculated as:

$$LE = sqrt((x^P_{CG} - x^T_{CG})^2 + (y^P_{CG} - y^T_{CG})^2)/l \tag{5}$$

where l represents the length of the long axis of the brain model.

The ICC measures the overall differences between the reconstructed and reference EIT images. We define it as:

$$ICC = \frac{\sum_{i=1}^{m} (\delta\rho_i^{Rec} - \delta\rho_i^{Ref})}{(\sum_{i=1}^{m} \delta\rho_i^{Ref})/m} \tag{6}$$

where $\delta\rho_i^{Rec}$ and $\delta\rho_i^{Ref}$ are the impedance changes of the i *th* element in the reconstructed and reference EIT images, respectively.

C. ANIMAL MODELS

This study was approved by the Animal Research Ethics Committee of the Air Force Medical University and conducted following its guidelines on animal experiments. Twelve rabbits from Switzerland (half male and half female, weighing approximately 3.0 kg, Xi'an, China) were randomly divided into two groups ($k = 6$ for each group). The rabbits were anesthetized with Isoflurane (induction 5% and maintenance 2%). As shown in Fig. 3(a), Group 1 consists of normal control rabbits. We placed eight electrodes on the scalp of the rabbits after removing the hair on their heads. With this model, we could image the entire cerebral impedance changes through brain EIT after infusing mannitol. As shown in Fig. 3(b), a plastic sheet is inserted between the scalp and the skull of the rabbits so that the intracranial signal can be shielded; thus, we could use EIT to solely measure the

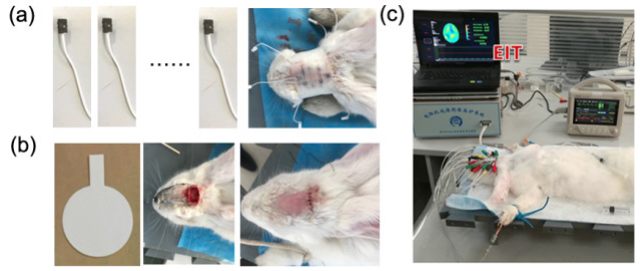

FIGURE 3. Illustration of animal models. (a) Scalp electrodes and rabbit model for monitoring the dehydration of the entire brain, (b) Insulating material and rabbit model for monitoring the dehydration of scalp, (c) Image of monitoring brain dehydration and physiological parameters of the rabbits.

dehydration of the scalp. Fig. 3(c) shows the image of the animal experiments, in which we utilized EIT and physiological monitoring to detect the brain dehydration and significant physiological parameters of the rabbits after mannitol was infused with a dosage of 0.3 g/kg [7]. All animal experiments were conducted under the room temperature.

D. D ANIMAL EXPERIMENT

In animal experiments, we first evaluate the contribution of the impedance changes of the scalp to the changes of EIT signals during mannitol dehydration treatments. With the models shown in Figs. 3(a) and (b), we obtained the TBV of the dehydrations of the scalp and entire brain tissues and denoted them by TBV_{scalp} and TBV_{all}, respectively. The contribution of scalp dehydration to the EIT signal can be estimated as $\mathrm{TBV}_{scalp}/\mathrm{TBV}_{all}$.

Second, we reconstructed the EIT images of the dehydration of the scalp and entire brain. With the imaging results, we can compare the reconstructed intracranial impedance changes in the EIT images in the above two cases. Thus, the contribution of the scalp to the reconstructed values in the intracranial area of the EIT images could be estimated and used as a scale factor to further reduce the impact of scalp dehydration.

IV. THE WEIGHTING ALGORITHM FOR REDUCING INFLUENCE OF SCALP DEHYDRATION

In the image reconstruction of EIT, the impedance changes $\delta\rho$ and measured EIT voltages δU have a linear relationship [23]:

$$\delta U = J_M \delta\rho \tag{7}$$

where J_M is the modified sensitivity matrix, proposed in [17], used to optimize the imaging results of the large-area resistive perturbation in dehydration treatments. As (7) is highly ill-posed, we solve this equation by converting it as follows:

$$\delta\rho = \arg\min ||\delta U - J_M\delta\rho||^2 + \lambda||R\delta\rho||^2 \tag{8}$$

Based on (8), the brain impedance changes during the dehydration treatments can be calculated as:

$$\delta\rho_{all} = (J_M^T J_M + \lambda R^T R)^{-1} J_M^T \delta U = \delta\sigma_{intra} + \delta\sigma_{scalp} \tag{9}$$

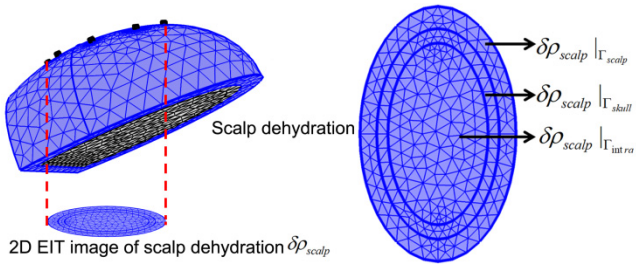

FIGURE 4. Illustration of a 2D tomographic EIT image of scalp dehydration.

where $\delta\rho_{all}$, $\delta\rho_{scalp}$, and $\delta\sigma_{intra}$ represent the reconstructed impedance changes due to the dehydrations of the entire brain, scalp, and intracranial brain tissues, respectively.

As shown in Fig. 4, the reconstruction results of the scalp dehydration $\delta\rho_{scalp}$ covers all the imaging domains in the EIT images. Therefore, we can represent the reconstruction results of the scalp as:

$$\delta\rho_{scalp} = \begin{cases} \delta\rho_{scalp}|_{\Gamma_{scalp}} \\ \delta\rho_{scalp}|_{\Gamma_{skull}} \\ \delta\rho_{scalp}|_{\Gamma_{intra}} \end{cases} \tag{10}$$

where $\delta\rho_{scalp}|_{\Gamma_{scalp}}$, $\delta\rho_{scalp}|_{\Gamma_{skull}}$, and $\delta\rho_{scalp}|_{\Gamma_{intra}}$ represent the reconstructed impedance changes in the scalp, skull, and parenchyma areas in the 2D EIT images, respectively, due to scalp dehydration. With (10), $\delta\rho_{All}$ can be rewritten as:

$$\begin{aligned} \delta\rho_{all} &= \begin{cases} \delta\rho_{scalp}|_{\Gamma_{scalp}} \\ \delta\rho_{scalp}|_{\Gamma_{skull}} \\ \delta\rho_{all}|_{\Gamma_{intra}} \end{cases} \\ s.t.\ \delta\rho_{all}|_{\Gamma_{intra}} &= \delta\rho_{scalp}|_{\Gamma_{intra}} + \delta\rho_{intra}|_{\Gamma_{intra}} \end{aligned} \tag{11}$$

In the modified algorithm, we take $B = (J_M^T J_M + \lambda R^T R)^{-1} J_M^T$ as the reconstruction matrix. Therefore, (9) can be rewritten as:

$$\delta\rho_{all} = B\delta U \tag{12}$$

From (12), we know that the elements in the i th column of B determine the reconstructed value of the i th element. Therefore, to reduce the impact of scalp dehydration and estimate $\delta\rho_{intra}|_{\Gamma_{intra}}$, we construct a diagonal matrix $W \in R^{m*m}$ to weight the elements in the i th column of B. Accordingly, the modified reconstruction results can be rewritten as:

$$\delta\rho'_{all} = WB\delta U \tag{13}$$

Based on the CT of the patients, we can obtain their EIT-CT images so that the location of the elements can be determined. With the above priori, the i th diagonal element of W can be set as:

$$w_i = \begin{cases} 0 & if\ e_i \in \Gamma_{scalp}\ or\ e_i \in \Gamma_{skull} \\ 1 - \dfrac{mean(\delta\rho_{scalp}|_{\Gamma_{intra}})}{mean(\delta\rho_{all}|_{\Gamma_{intra}})} & if\ e_i \in \Gamma_{intra} \end{cases} \tag{14}$$

where w_i represents the *i th* diagonal element of W, and e_i is the *i th* element of $\delta\rho$. For the elements in the scalp and skull areas of the EIT images, $w_i = 0$. Therefore, the unwanted reconstruction results $\delta\rho_{scalp}|_{\Gamma_{scalp}}$ and $\delta\rho_{scalp}|_{\Gamma_{skull}}$ can be eliminated. For the reconstruction results in the intracranial area of the EIT images, we can estimate the contribution of the scalp impedance changes to the reconstructed values in Γ_{intra} from the results of the animal experiments. Thus, we set $w_i = 1 - \frac{mean(\delta\rho_{scalp}|_{\Gamma_{intra}})}{mean(\delta\rho_{all}|_{\Gamma_{intra}})}$ to reduce the impact of the scalp on the imaging results in Γ_{intra}.

After the above processing, the weighted solution $\delta\rho'_{all}$ will be approximately equal to $\delta\sigma_{intra}$.

V. RESULTS

A. RESULTS OF EVALUATION EXPERIMENTS

In this part, we show the results of the simulation and animal experiments for evaluating the impact of scalp dehydration on the monitoring results of brain EIT in mannitol dehydration.

1) RESULTS OF SIMULATION EXPERIMENTS

In the simulation experiments, we first compared the detection sensitivity of brain EIT with and without scalp impedance changes based on the 3D simulation rabbit head model. As shown in Fig. 5(a), the impedances of the scalp and intracranial brain tissues are increased by 10% to simulate the dehydration. And in Fig. 5(b), we only increased the impedance of intracranial tissues. The excitation currents were injected via the electrodes 1 and 5. As shown in Figs. 5(c) and (d), we compare and show the plots of the EIT current density in the brain with and without the scalp impedance changes. In the plots, the red and blue colors indicate the large and small amplitudes of the current density, respectively. The results show that without an increase in the scalp impedance, the excitation current magnitude inside the brain is higher. As EIT is more sensitive to intracranial resistive perturbation with an increase in the excitation currents [24], scalp impedance changes could affect EIT while detecting intracranial dehydration. With the results shown in Fig. 4, we calculated the average values of the intracranial current density (CD) in the above two cases; they were found to be 0.28 and 0.32 A/m^2, respectively. Therefore, the detection sensitivity of brain EIT decreased by approximately 12.5% due to scalp impedance changes.

Fig. 6 shows the imaging results of the EIT for the dehydration treatments with and without scalp impedance changes. In Figs. 6(a) and (c), spheres with a radius of 0.125 cm are inserted at different locations of the simulation head model. The resistivity of the targets was set to 6.71 Ω/m, which is the same as that of brain parenchyma. With the spheres, we could simulate that there was no dehydration in these areas. Figs. 6(b) and (d) show their imaging results with and without scalp impedance changes, respectively.

The results show that when the scalp exhibits impedance changes, the image contrast decreases, which is not conducive to distinguishing areas with bad dehydration. In Fig. 7, we compare the IC, LE, and ICC of the imaging results obtained with and without scalp impedance changes. Due to the impedance changes of the scalp, the IC decreased

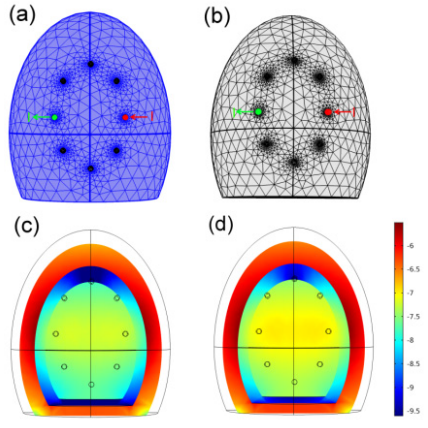

FIGURE 5. Comparison of the current density inside the brain with and without scalp impedance changes. (a): Simulation rabbit head model with increase of scalp impedance. (b): Simulation of rabbit head model without scalp impedance changes. The red and blue arrows here represent the injection of excitation currents. (c) The distribution of current density with scalp impedance changes. (d) The distribution of current density without scalp impedance changes.

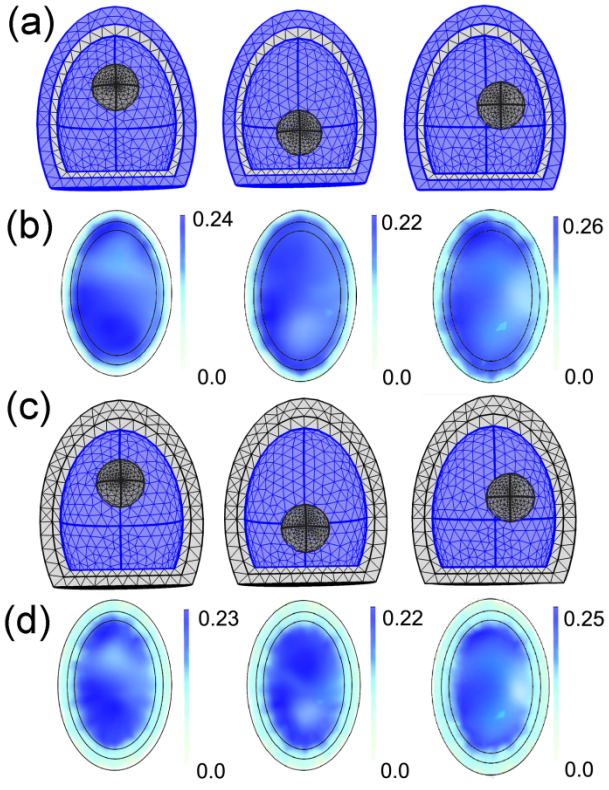

FIGURE 6. Imaging results of intracranial dehydration with and without scalp impedance changes. (a) Simulation of dehydration of the entire brain, (b) Imaging results of brain dehydration with scalp impedance changes, (c) Simulation of dehydration of intracranial brain tissues, (d) Imaging results of brain dehydration without scalp impedance changes.

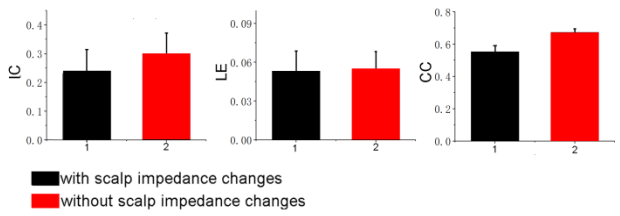

FIGURE 7. Quantitative evaluation results of the reconstructed EIT images with and without scalp impedance changes. IC, LE, and CC are the image contrast, location error, and correlation coefficient of the images, respectively.

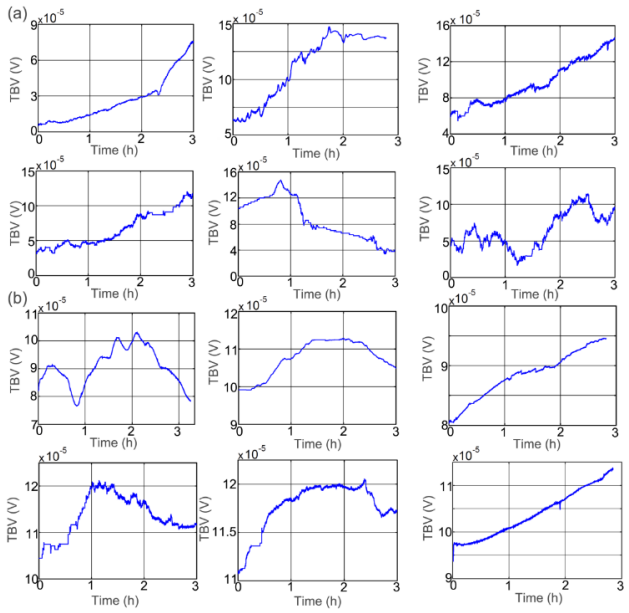

FIGURE 8. Plots of total boundary voltage (TBV) changes during the dehydrations of the entire brain (a) and the scalp (b).

from 0.303 ± 0.09 to 0.243 ± 0.08 and the ICC from 0.653 ± 0.02 to 0.573 ± 0.05. The LE had no obvious changes. Based on the quantitative evaluation results, we found that an increase in the scalp impedance can to some extent reduce the image quality of brain EIT.

2) RESULTS OF ANIMAL EXPERIMENTS

In the animal experiments, based on the models shown in Figs. 3(a) and (b), we first measured the voltage changes due to the dehydrations of the scalp and the entire brain using EIT. Fig. 8 shows the TBV curves in the above cases.

Fig. 8(a) shows the TBV curves for the dehydration of the scalp, denoted by TBV_{scalp}. Fig. 8(b) shows the TBV curves for the dehydration of the entire brain, denoted by TBV_{all}. Based on the above results, we calculated the maximum changes in the TBV in the two cases, as listed in Table 1. From the results, we found that the contribution of the impedance changes of the scalp to the EIT signals is approximately 16.7%. Therefore, it would be more accurate to assess the effects of dehydration inside the brain if we can eliminate the measurements of scalp dehydration.

TABLE 1. Maximum changes in TBV in the monitoring of intracranial and scalp dehydration.

The order of rabbits	$\mathrm{TBV}_{all}^{\max}$ ($\times 10^{-5}$ V)	$\mathrm{TBV}_{scalp}^{\max}$ ($\times 10^{-5}$ V)
1	8.85	1.83
2	9.44	1.37
3	8.69	1.36
4	8.26	1.20
5	7.45	1.04
6	7.22	1.60
Mean±std	8.35±0.82	1.40±0.28

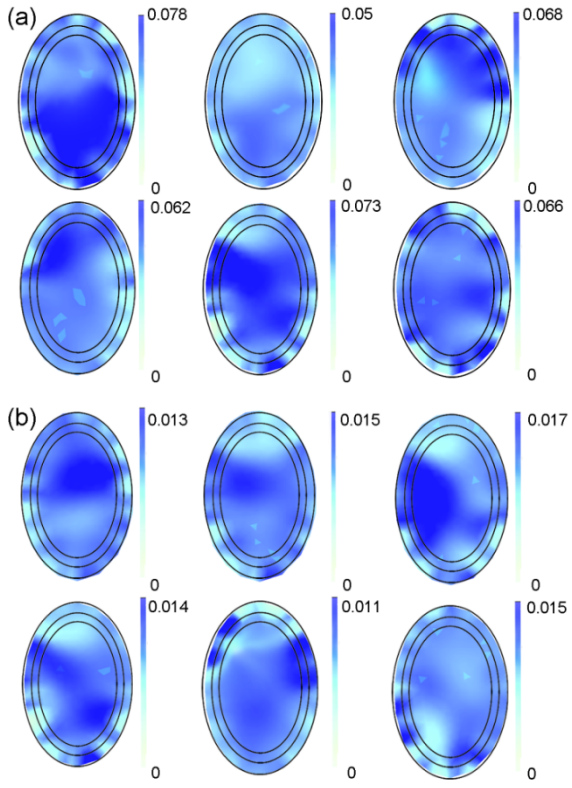

FIGURE 9. Imaging results of dehydration of the entire brain (a) and scalp (b) in animal experiments.

Based on the above measurements, shown in Fig. 9, we reconstructed the impedance changes of the entire brain tissues and the scalp at the time when the effects of the dehydration treatments reached their peaks. We denote the reconstruction results in Fig. 8(a) and (b) as $\delta\rho_{all}$ and $\delta\rho_{scalp}$, both of which cover all the domains in the 2D EIT images including the scalp, skull, and intracranial areas. With $\delta\rho_{all}$ and $\delta\rho_{scalp}$, $\delta\rho_{all}|_{\Gamma_{intra}}$ and $\delta\rho_{scalp}|_{\Gamma_{intra}}$ could be obtained. The averages of $\delta\rho_{all}|_{\Gamma_{intra}}$ and $\delta\rho_{scalp}|_{\Gamma_{intra}}$ are 0.092 and 0.61 Ω/m; from this, we find that the contribution of scalp dehydration to the reconstructed impedance changes in the intracranial area in EIT images is approximately 15.2%.

With this result, we can set the weighting coefficient corresponding to the elements in the intracranial areas as 0.848 (1-0.152) to reduce the reconstructed impedance changes due to scalp dehydration.

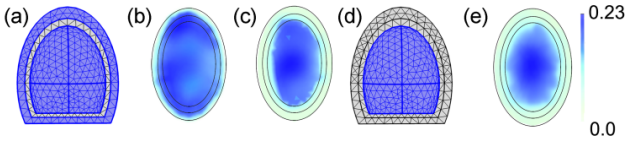

FIGURE 10. Imaging results of brain dehydration with and without scalp impedance changes using different methods. (a) Simulation of brain dehydration with scalp impedance changes, (b), (c) Reconstruction results of brain dehydration with scalp impedance changes using the previous and the proposed algorithm, (d) Simulation of brain dehydration without scalp impedance changes, (e) Reconstruction results of brain dehydration without scalp impedance changes using the previous algorithm.

B. RECONSTRUCTION RESULTS OF THE MODIFIED ALGORITHM

In this part, we report the results of simulation experiments conducted to test the performance of the weighting algorithm. First, in Fig. 10, we tested whether the proposed algorithm could reduce the reconstruction results of scalp dehydration in the EIT images. In Figs. 10(a) and (d), we simulated the brain dehydration with and without scalp impedance changes, respectively. The impedance of the scalp and intracranial brain tissues were also increased by 10%, the same setting as in the above simulation experiments. In Figs. 10 (b) and (c), the EIT images of brain dehydration with scalp impedance changes were reconstructed using the previous and proposed algorithms. From the imaging results, we find that with the weighting matrix, the unwanted reconstructed values in the scalp and skull areas are eliminated. Fig. 10(e) shows the reconstruction results of intracranial dehydration without scalp impedance changes based on the previous algorithm. The ARVs of the imaging results, shown in Figs. 10(b), (c), and (e), are 0.208, 0.186, and 0.162 Ω, respectively. In reconstruction results of the proposed algorithm, the ARV due to scalp dehydration decreased from 0.046 to 0.014 Ω. So, 69.6% ((0.046-0.014)/0.046) of the reconstruction values due to scalp dehydration in EIT images were removed.

Then, in Fig. 11, we tested whether the proposed method could improve the image quality of brain EIT in imaging bad dehydration areas inside the brain. In Fig. 11(a), we simulated areas inside the brain with bad dehydration. We then reconstructed the EIT images shown in Figs. 11(b) and (c) with the previous and modified algorithms, respectively. The imaging results show that the reconstructed areas with bad dehydration in the EIT images obtained by our method were more obvious. Based on the imaging results, we compared their IC. The IC values for the images in Fig. 11(b) and (c) were 0.243 ± 0.08 and 0.294 ± 0.09, respectively. The IC was improved about 21.0% with the proposed algorithm. Therefore, our proposed method could enhance the image quality of EIT with disturbance from the dehydration of scalp during the imaging of brain dehydration.

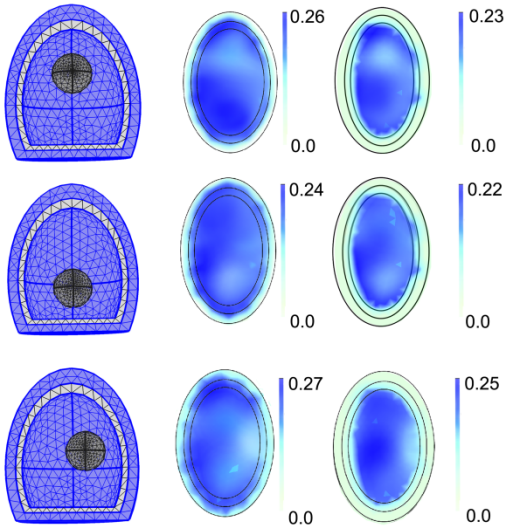

FIGURE 11. Imaging results of areas with bad dehydration effects inside the brain using the previous and proposed algorithms. (a) Simulation of areas with bad dehydration effects, (b) Reconstruction results using the previous algorithm, (c) Reconstruction results using the proposed method.

VI. DISCUSSION

Monitoring intracranial dehydration treatments using brain EIT is a promising approach as it provides references for the rational use of drugs. In this novel application, in addition to brain tissues, the scalp exhibits impedance changes during the dehydration. which can affect the EIT monitoring results. The EIT signals corresponding to the dehydrations of scalp and intracranial tissues change simultaneously and cannot be distinguished from frequent characteristics. To enable EIT to reflect intracranial dehydration more accurately, we evaluated and proposed a method to reduce the influence of scalp dehydration.

Based on the results of evaluation experiments, we found that in the monitoring of intracranial dehydration, scalp would not cause fatal errors in the EIT results but would influence the results of EIT in following aspects:

(1) For the imaging results of EIT, an increase in the scalp impedance due to dehydration would reduce the amount of current flowing to the brain, which could lead to reduced sensitivity of brain EIT to intracranial impedance changes. In addition, the scalp impedance changes would to some extent affect EIT in the imaging areas with bad dehydration effects.

(2) For EIT signals, the voltage changes due to scalp dehydration account for approximately 16.7%. Therefore, EIT would reflect intracranial dehydration with improved precision if we can reduce the impact of scalp dehydration.

In this study, a weighting algorithm was proposed to preliminarily reduce the impact of scalp dehydration. In this algorithm, to eliminate the unwanted reconstructed values of the elements in the scalp and skull areas of the EIT images, the weighting coefficients corresponding to these elements were set to 0. From the results of animal experiments, the contribution of scalp dehydration to the reconstructed values in the intracranial areas of the EIT images was estimated to be 0.152. Therefore, the scale parameter for the elements in the intracranial areas was set as 0.848 (1-0.152) to make the

reconstruction results only relate to the dehydration of the tissues inside the brain.

With the above processing, the impact of scalp dehydration could be understood and effectively reduced. However, there were some several limitations in this study. First, in the animal experiments, we inserted an insulating material between the scalp and skull of the rabbits for solely measuring the dehydration of the scalp. The plastic sheet did not cover the entire head so the results may not be completely accurate. Secondly, we estimated the contribution of scalp to the intracranial impedance changes in the EIT images and utilized this statistical result to reduce the impact of scalp dehydration in the modified algorithm. However, there might be measurement errors which would make the algorithm inaccurate. In the future, we will increase the number of samples in the animal experiments for the more accurate estimation. Thirdly, the performance of the proposed method was only verified based on simulation experiments, we will construct more complex animal models to test its performance and we would try to apply it to 3D imaging [25].

VII. CONCLUSION

Based on the experimental results of this study, we can conclude that in the application of dynamic brain EIT to monitoring intracranial dehydration treatments, the dehydration of scalp will to some extent reduce the detection sensitivity of brain EIT, decrease the image quality and cause unwanted changes in EIT measurements, which were not favored in locating the area with bad dehydration and evaluating the degree of the dehydration of tissues inside the brain. To reduce the impacts of scalp, we propose a novel weighting algorithm using the priori of spatial distribution of brain structures and the statistical results of contribution of scalp dehydration to reconstructed values in intracranial areas of EIT images obtained in animal experiments. With this algorithm, the reconstructed values in EIT images due to dehydration of scalp were suppressed and it could ensure the imaging results of EIT to reflect distribution of intracranial dehydration more accurately.

ACKNOWLEDGEMENT

(Haoting Li, Lu Cao, and Canhua Xu contributed equally to this work.)

REFERENCES

[1] I. Frerichs, "Electrical impedance tomography (EIT) in applications related to lung and ventilation: A review of experimental and clinical activities," *Physiol. Meas.*, vol. 21, no. 2, pp. R1–R21, May 2000.
[2] A. Adler and A. Boyle, "Electrical impedance tomography: Tissue properties to image measures," *IEEE Trans. Biomed. Eng.*, vol. 64, no. 11, pp. 2494–2504, Nov. 2017.
[3] R. Bayford and A. Tizzard, "Bioimpedance imaging: An overview of potential clinical applications," *Analyst*, vol. 137, no. 20, p. 4635, 2012.
[4] D. Djajaputra, "Electrical impedance tomography: Methods, history and applications," *Med. Phys.*, vol. 32, no. 8, p. 2731, Aug. 2005.
[5] R. M. Chesnut, G. Petroni, and C. Rondina, "Intracranial-pressure monitoring in traumatic brain injury," vol. 369, no. 25, p. 2465, 2013.
[6] P. Le Roux, "Intracranial pressure monitoring and management," in *Translational Research in Traumatic Brain Injury*, D. Laskowitz and G. Grant, Eds. Boca Raton, FL, USA, 2016.
[7] P. Czupryna, A. Moniuszko-Malinowska, S. Grygorczuk, S. Pancewicz, J. Dunaj, M. Król, K. Borawski, and J. Zajkowska, "Effect of a single dose of mannitol on hydration status and electrolyte concentrations in patients with tick-borne encephalitis," *J. Int. Med. Res.*, vol. 46, no. 12, pp. 5083–5089, Dec. 2018.
[8] O. W. Sakowitz, J. F. Stover, A. S. Sarrafzadeh, A. W. Unterberg, and K. L. Kiening, "Effects of mannitol bolus administration on intracranial pressure, cerebral extracellular metabolites, and tissue oxygenation in severely head-injured patients," *J. Trauma*, vol. 62, no. 2, pp. 292–298, Feb. 2007.
[9] F. Fu, B. Li, M. Dai, S.-J. Hu, X. Li, C.-H. Xu, B. Wang, B. Yang, M.-X. Tang, X.-Z. Dong, Z. Fei, and X.-T. Shi, "Use of electrical impedance tomography to monitor regional cerebral edema during clinical dehydration treatment," *PLoS ONE*, vol. 9, no. 12, Dec. 2014, Art. no. e113202.
[10] B. Yang, B. Li, C. Xu, S. Hu, M. Dai, J. Xia, P. Luo, X. Shi, Z. Zhao, X. Dong, Z. Fei, and F. Fu, "Comparison of electrical impedance tomography and intracranial pressure during dehydration treatment of cerebral edema," *NeuroImage, Clin.*, vol. 23, Jan. 2019, Art. no. 101909.
[11] H. Li, H. Ma, B. Yang, C. Xu, L. Cao, X. Dong, and F. Fu, "Automatic evaluation of mannitol dehydration treatments on controlling intracranial pressure using electrical impedance tomography," *IEEE Sensors J.*, vol. 20, no. 9, pp. 4832–4839, May 2020.
[12] G. Boverman, T.-J. Kao, X. Wang, J. M. Ashe, D. M. Davenport, and B. C. Amm, "Detection of small bleeds in the brain with electrical impedance tomography," *Physiol. Meas.*, vol. 37, no. 6, pp. 727–750, Jun. 2016.
[13] O. Gilad and D. S. Holder, "Impedance changes recorded with scalp electrodes during visual evoked responses: Implications for electrical impedance tomography of fast neural activity," *NeuroImage*, vol. 47, no. 2, pp. 514–522, Aug. 2009.
[14] M. Faulkner, M. Jehl, K. Aristovich, J. Avery, A. Witkowska-Wrobel, and D. Holder, "Optimisation of current injection protocol based on a region of interest," *Physiol. Meas.*, vol. 38, no. 6, pp. 1158–1175, Jun. 2017.
[15] J.-B. Li, M.-X. Tang, X.-Z. Dong, C. Tang, M. Dai, G. Liu, X.-T. Shi, B. Yang, C.-H. Xu, F. Fu, and F.-S. You, "A new head phantom with realistic shape and spatially varying skull resistivity distribution," *IEEE Trans. Biomed. Eng.*, vol. 61, no. 2, pp. 254–263, Feb. 2014.
[16] A. D. Liston, R. H. Bayford, A. T. Tidswell, and D. S. Holder, "A multi-shell algorithm to reconstruct EIT images of brain function," *Physiol. Meas.*, vol. 23, no. 1, pp. 105–119, Feb. 2002.
[17] H. Li, L. Cao, C. Xu, B. Liu, B. Yang, X. Dong, and F. Fu, "Optimized method for electrical impedance tomography to image large area conductive perturbation," *IEEE Access*, vol. 7, pp. 140734–140742, 2019.
[18] H. Li, R. Chen, C. Xu, B. Liu, M. Tang, L. Yang, X. Dong, and F. Fu, "Unveiling the development of intracranial injury using dynamic brain EIT: An evaluation of current reconstruction algorithms," *Physiol. Meas.*, vol. 38, no. 9, pp. 1776–1790, Aug. 2017.
[19] C. Xu, M. Dai, F. You, X. Shi, F. Fu, R. Liu, and X. Dong, "An optimized strategy for real-time hemorrhage monitoring with electrical impedance tomography," *Physiol. Meas*, vol. 32, no. 5, p. 585, May 2011.
[20] C. Tang, F. You, G. Cheng, D. Gao, F. Fu, G. Yang, and X. Dong, "Correlation between structure and resistivity variations of the live human skull," *IEEE Trans. Biomed. Eng.*, vol. 55, no. 9, pp. 2286–2292, Sep. 2008.
[21] Z. Xu, Y. Jiang, B. Wang, Z. Huang, H. Ji, and H. Li, "Sensitivity distribution of CCERT sensor under different excitation patterns," *IEEE Access*, vol. 5, pp. 14830–14836, 2017.
[22] A. Adler, J. H. Arnold, R. Bayford, A. Borsic, B. Brown, P. Dixon, T. J. C. Faes, I. Frerichs, H. Gagnon, Y. Gärber, B. Grychtol, G. Hahn, W. R. B. Lionheart, A. Malik, R. P. Patterson, J. Stocks, A. Tizzard, N. Weiler, and G. K. Wolf, "GREIT: A unified approach to 2D linear EIT reconstruction of lung images," *Physiol. Meas.*, vol. 30, no. 6, pp. S35–S55, Jun. 2009.
[23] D. Liu, D. Smyl, and J. Du, "A parametric level set-based approach to difference imaging in electrical impedance tomography," *IEEE Trans. Med. Imag.*, vol. 38, no. 1, pp. 145–155, Jan. 2019.
[24] W. R. Fan and H. X. Wang, "Maximum entropy regularization method for electrical impedance tomography combined with a normalized sensitivity map," *Flow Meas. Instrum.*, vol. 21, no. 3, pp. 277–283, Sep. 2010.
[25] B. Grychtol, B. Müller, and A. Adler, "3D EIT image reconstruction with GREIT," *Physiol. Meas.*, vol. 37, no. 6, pp. 785–800, Jun. 2016.